Journal of Hydrology: Regional Studies 38 (2021) 100938

Contents lists available at ScienceDirect

Journal of Hydrology: Regional Studies

journal homepage: www.elsevier.com/locate/ejrh

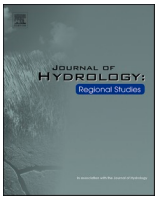

Revealing the spatio-temporal characteristics of drought in Mozambique and their relationship with large-scale climate variability

Ronnie J. Araneda-Cabrera [a,*], María Bermudez [b], Jerónimo Puertas [a]

[a] *Water and Environmental Engineering Group (GEAMA), University of A Coruña, Civil Engineering School, Campus de Elviña, 15008 A Coruña, Spain*

[b] *Environmental Fluid Dynamics Group, Andalusian Institute for Earth System Research, University of Granada, Av. Del Mediterráneo s/n, 18006 Granada, Spain*

ARTICLE INFO

Keywords:
Drought
Standardized Precipitation and Evapotranspiration Index (SPEI)
Regionalization
Trend
Persistence
Teleconnections
Climatic indices

ABSTRACT

Study region: Mozambique.
Study focus: Mozambique does not currently have the necessary tools for systematic monitoring and forecasting of drought at a subnational scale. The purpose of this study was to characterize drought conditions and trends throughout the country and to evaluate the influence of major climatic drivers on drought events (period 1950–2019). Drought conditions were studied by means of the Standardized Precipitation and Evapotranspiration Index (SPEI) and run theory. The principal component analysis technique and the k-means clustering method were applied for defining homogenous drought regions. The Mann-Kendall trend test and Rescaled Range statistical analysis were used for defining the temporal characteristics of drought. The cross-correlation method, a spectral analysis based on the Fast Fourier Transform and a cross-wavelet analysis, were used to identify possible climate drivers. The results are ultimately intended to contribute to the development of a drought monitoring system in this country.
New hydrological insights for the region: Three homogeneous drought regions can be defined in Mozambique. The South and Centre regions showed more intense and severe drought events. In all regions, a significant trend towards a higher incidence of droughts and long-term a persistence were found. El Niño-Southern Oscillation and Darwin Sea Level Pressure anomalies were identified as significant drivers of drought variability, especially in the southern regions. These climate indices can be used as predictors in drought forecasting models.

1. Introduction

Droughts are among the most common natural phenomena worldwide, and can occur anywhere under any climate regime (Bryant et al., 2005; Sheffield and Wood, 2012). However, they constitute one of the least understood natural hazards due to their complexity and difficulties in quantification (Hagenlocher et al., 2019). The effects of droughts can be felt in chains of energy production, food, water supply, etc., yet are generally detected when the consequences of the phenomenon are difficult to mitigate, and thus droughts constitute the disaster that causes the greatest socioeconomic losses worldwide (WMO, 2006). In addition, the effects of droughts are

* Corresponding author.
E-mail address: ronnie.aranedac@udc.es (R.J. Araneda-Cabrera).

https://doi.org/10.1016/j.ejrh.2021.100938
Received 7 January 2021; Received in revised form 29 September 2021; Accepted 30 September 2021
Available online 19 October 2021

expected to worsen in the coming decades as a result of climate change. Changes in spatial-temporal patterns of precipitation and extreme temperatures are likely to make droughts more recurrent (Mishra and Singh, 2011). As stated by the IPCC (2014), there are trends of increasing intensities and frequencies of droughts around the world, with arid and semi-arid areas possibly being the most affected. This might invalidate traditional methods for examining the impact of environmental factors on drought, based as they are on the assumption of stationarity (Jehanzaib et al., 2020). Specific spatiotemporal drought assessments at regional or local levels are needed for reliable decision-making in the context of adaptation planning to future climate conditions (see, e.g., Jehanzaib and Kim, 2020; Kim and Jehanzaib, 2020; and the references therein).

According to Wilhite et al. (2000), one of the first steps for drought assessment and management in a given zone (country or river basin) should be a spatial division into regions according to drought characteristics. The techniques of hierarchical and non-hierarchical clustering (Santos et al., 2010; Vicente-Serrano, 2006a) and Principal Component Analysis (Agutu et al., 2017; Lovino et al., 2014; Vicente-Serrano, 2006b) can be applied directly to drought indicators for identifying homogenous drought regions. The next steps should be aimed at developing a drought monitoring system to create early warnings of emerging drought conditions. The temporal variability of droughts in the area under analysis must be studied to accomplish this objective. The historical drought variability is usually analysed by means of a technique such as run theory (Yevjevich, 1969), accompanied by trend and persistence tests of the drought characteristics (Ayantobo et al., 2017; Huang et al., 2016; Zambreski et al., 2018). The subsequent step is then to forecast droughts. Thus, it is necessary to understand the climate drivers that trigger drought events in the region and to use this teleconnection information as a forecasting tool. To achieve this goal, methods such as cross-correlation (Araneda-Cabrera et al., 2021a; Hair et al., 1998) and various spectral analysis applied to climate indices and drought indicators have become popular as a means of identifying appropriate drought predictors (El Kenawy et al., 2016; Espinosa et al., 2019; Fleming et al., 2002; Zeleke et al., 2017).

A large number of drought indicators serve as a basis for these analyses (Svodova et al., 2016). The Palmer Drought Severity Index (PDSI) (Palmer, 1965) is widely used due to its versatility and effectiveness (Alley, 1984; Nam et al., 2015; Quiring and Papakryiakou, 2003). The Standardized Precipitation Index (SPI) (McKee et al., 1993), currently recommended by the World Meteorological Organization, uses rainfall series to define drought periods and has also been used widely in studies around the world (Ayantobo et al., 2017; Stagge et al., 2017). One of its main advantages, compared to the PDSI, is that it can be computed for multiple time scales, which allows the assessment of water availability according to the process under consideration (e.g., 3-month SPI provides a seasonal estimation of precipitation, whereas 12-month SPI reflects long-term precipitation patterns) (Guttman, 1999, 1998). More recently, the Standardized Precipitation and Evaporation Index (SPEI) was introduced by Vicente-Serrano et al. (2010a, 2010b). Its versatility is similar to that of the SPI and it has the advantage of considering both precipitation and evapotranspiration. Vicente-Serrano et al. (2010a, 2010b) found that SPEI had a better performance than SPI and PDSI under global warming scenarios since it could reflect the increase in drought severity associated with higher water demand due to evapotranspiration. However, the need for long-term and high-quality input data is often a problem for the application of these indicators, especially in poorly monitored regions (Easterling, 2013). In recent years, global databases such as Climate Research Unit (CRU) (Harris et al., 2014), TerraClimate (Abatzoglou et al., 2018) and the Global Precipitation Climatology Centre (GPCC) (Rudolf et al., 2011) have emerged as alternative data sources, showing good performance in drought studies (Araneda-Cabrera et al., 2021b, 2020; Lovino et al., 2014).

In this study, we evaluate the spatiotemporal distribution of drought in Mozambique, and explore its relationships with large-scale climate variability. This country is one of the poorest in the world, highly dependent on rain-fed agriculture, and very prone to droughts. It has very little water infrastructure and a lack of monitoring systems, so its resilience to extreme hydrological events is very low (Osbahr et al., 2008). To the best of the authors' knowledge, there is a lack of comprehensive drought studies at the national level that might provide the basis for the development of national drought monitoring and forecasting systems. The possibility of drought forecasting has only been explored in small parts of the country, with a focus on the Limpopo Basin (Dutra et al., 2013; Seibert et al., 2017; Trambauer et al., 2015, 2014). Climate variability has also been studied in specific regions as part of vulnerability and adaptation assessments (Eriksen and Silva, 2009; Macarringue et al., 2017; Osbahr et al., 2008; Uele et al., 2017). Similarly, the relationship between droughts and climate indices has not been widely analysed in the country. Manhique et al. (2011) note that El Niño-Southern Oscillation (ENSO) appears to play a significant role in the inter-annual frequency of the main summer rainfall over Mozambique. However, other climate indices, such as Darwin sea level pressure, have been shown to influence the climate in neighbouring countries (Manatsa et al., 2008a, 2008b).

The main objective of the current study is to characterize drought conditions and trends over Mozambique between 1950 and 2019, and to identify the influence of large-scale climatic drivers on drought events. We follow a five-step methodology (described in Section 2) of general applicability (i.e., one that could be used in any other country or region worldwide) comprising drought regionalization, characterization, trend analysis, long-term dependence, and cross-dependence with climatic factors. Given that Mozambique is heavily reliant on agriculture, the analysis focuses on persistent drought, which can affect agricultural production and food security. In this way, the results are intended to be of practical value to water managers and users. The ultimate aim is to support drought management planning with tools that enable better monitoring and prediction of risk at the regional scale.

2. Materials and methodology

The methodology developed in this study involves the following steps: (1) the calculation of the SPEI drought index with a 12-month time scale (SPEI-12) for the period 1950–2019; (2) the application of Principal Component Analysis (PCA) analysis and the k-means clustering method to define homogeneous drought regions that follow the time patterns of the drought index series; (3) the characterization of the drought events according to run theory; (4) the application of the modified Mann-Kendall (MMK) trend test

method and the Rescaled Range (R/S) analysis to determine the temporal variability of droughts; and (5) the exploration of the relationships between the SPEI time series and several large-scale climate indices to find appropriate drought predictors. The cross-correlation method, the Fast Fourier Transform (FFT) and cross-wavelet analysis were used for this latter purpose. The methods employed at each step were complementary and not exclusive. Fig. 1 summarizes the steps in a methodological flow-chart.

The entire methodology was developed and computed using the R Software (RStudio Team, 2016). Specifically, we used the R package "SPEI" (Begueria and Vicente-Serrano, 2017), "stat" (Bolar, 2019), "lmomRFA", "trend" (Pohlert, 2020), "pracma" (Borchers, 2019), "tseries" (Trapletti et al., 2020), "stats" (developed by R Core Team and contributors worldwide) and "biwavelet" (Gouhier et al., 2016).

2.1. Study area

Mozambique covers an area of 801,000 km^2 (Fig. 2a). It is in the southern cone of Africa, one of the most drought-prone areas worldwide, where extreme hydrological events are expected to become more frequent and damaging due to climate change (Eriksen and Silva, 2009; Osbahr et al., 2008; Patt and Schröter, 2008). The climate is tropical, with a hot and rainy summer season from November to March (80% of the year's precipitation falls during this period), and a cool and dry winter season from April to October. The national average annual precipitation varies from 683 mm to 1276 mm, with the south and central west being the drier regions. The mean annual temperature varies from 23 °C to 25 °C, with the coastal regions of the centre and north of the country, plus the centre-west, being the warmest. The national average annual precipitation level has high interannual variability and has been below the average for most years in the past two decades (Fig. 2b). The average annual temperature has increased considerably over the last 20 years, where its anomalies have reached + 1 °C in relation to the period 1950–2019 (Fig. 2c). According to the International Disaster Database (EM-DAT, 2020), the drought events of 1987, 1991–1992, 1995 and 2016 were among the severest in the country, causing losses of 650 million dollars and affecting at least 24 million people (MunichRE, 2018). In these years, low precipitation and high temperature anomalies were observed.

Although rainfall volumes are higher in the north than in the south, droughts are a recurrent problem throughout the country, affecting the socio-economic activities and negatively impacting the quality of life of the population.

The National Directorate of Water (DNA) divides the country into three Regional Water Administrations—ARAs (Administração Regional de Águas)—which are responsible for managing extreme events such as droughts (Conselho de Ministros, 2020): South ARA, from the country's southern border to the Save river; Central ARA, running from the Save river to the Licungo river; and North ARA, comprising the territory from the Licungo river to the country's northern border with Tanzania (Fig. 2a). It should be noted that this division into 3 ARAs is very recent. Five ARAs were initially created in Mozambique as part of the 1991 Water Law, based on geographic and infrastructural conditions specific to their jurisdictional areas, prioritizing their institutional capacity (Inguane et al., 2014).

2.2. The Standardized Precipitation and Evapotranspiration Index (SPEI)

The SPEI was selected as a hydro-meteorological drought index due to its flexibility as a multi-scalar index (unlike the PDSI), and

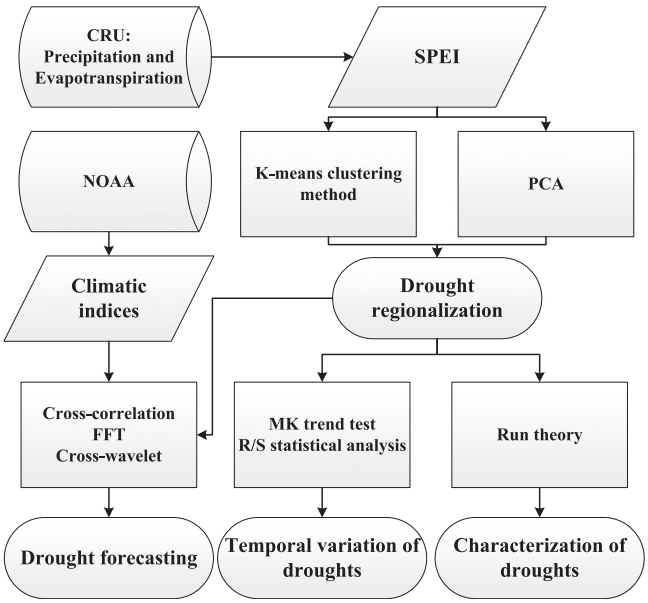

Fig. 1. Workflow of the overall methodology.

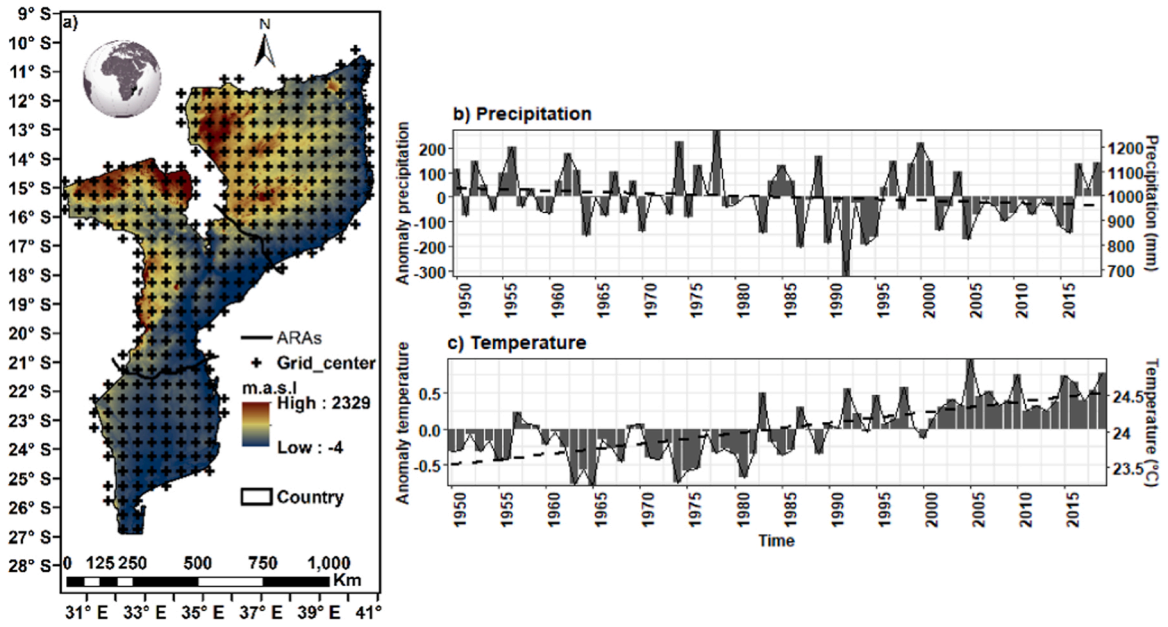

Fig. 2. a) Location of Mozambique and its topography with black marks that illustrate the Climate Research Unit (CRU) grid points (0.5° resolution) (Harris et al., 2014). Annual national average series of b) precipitation and c) temperature (solid lines) and anomalies with respect to the mean from 1950 to 2019 (bars). Dashed lines indicate linear trends.

because of its functionality under climate change conditions, in that it can account for the role of temperature increase in future drought conditions (unlike the SPI). The SPEI has been used successfully for drought monitoring in various studies around the world (Lovino et al., 2014; Meresa et al., 2016), and has been found to be more effective than other indices in capturing drought responses for ecological, agricultural, and hydrological applications (Vicente-Serrano et al., 2012).

The SPEI is based on the probability distribution of a long-term climatic water balance ($CWB = P - ETP$) time series, where P is the precipitation and ETP the potential evapotranspiration. It is typically computed by summing CWB over k months (similar to SPI), termed accumulation periods, and fitting these accumulated values to a parametric statistical distribution from which probabilities are standardized ($u = 0$, $\sigma = 1$). Given that the CWB series can have values below zero, a three-parameter distribution is needed to model them (Vicente-Serrano et al., 2010a). The three-parameter log-logistic distribution has been found to fit the CWB series very well across most of the world for most time scales (Vicente-Serrano et al., 2010b), so we have used this distribution here.

We utilized a 12-months accumulation ($k = 12$) to analyse the interannual variability of drought conditions. The choice of time scale is driven by the objectives of the study, which ultimately are to provide useful information for water managers and users for monitoring and forecasting drought. Drought at this scale can cause yield reductions for both rainfed and irrigated crops, posing a severe threat to food security in this country. It has also been seen in Mozambique that SPEI-12 is strongly correlated to SPEI at other scales, and that it is effective at detecting the country's historical drought records.(Araneda-Cabrera et al., 2021b). However, it should be noted that using this timescale presents some challenges, such as generating time series of independent measurements and capturing the whole drought cycle in a watershed or region.

Monthly P and ETP data were downloaded from the Climate Research Unit (CRU TS v. 4.04) (http://www.cru.uea.ac.uk/data) to compute the SPEI. CRU offers monthly climatic time series at a 0.5° resolution (≈ 55 km in the Equator) worldwide (Harris et al., 2014). At this resolution, a total of 343 time series of SPEI were computed in Mozambique (Fig. 2a). The time span of the analysis was from January 1950 to December 2019 (70 years).

For the purposes of this study, a drought event started when the SPEI took values lower than −1 and ended when its value returned to values higher than this threshold, which corresponds to moderate droughts according to the categories in McKee et al. (1993). In addition, to ensure that drought events were independent of each other, and to group mutually dependent droughts, we used the inter-event time method introduced by Zelenhasić and Salvai (1987), which is still widely applied in the recent literature (e. g. Liu et al., 2020; Rivera et al., 2021). Drought events were designated as independent if the inter-event time lasted more than 2 months (i.e., 2 consecutive months above the proposed drought threshold); while a drought qualified as an event if it lasted more than 2 months. The events were characterized according to run theory, explained in detail in Yevjevich (1969). The intensity (Int) is the minimum monthly value that is reached by the index throughout the event, the duration (Du) is the number of months that the event lasts, and the severity (Sev) is computed as the sum of monthly SPEI values throughout the event.

2.3. Drought regionalization

Principal component analysis (PCA) was used to identify drought patterns in the SPEI series, and hence define homogeneous

regions with similar drought variability and characteristics. It has been widely used for similar regionalization purposes in other parts of the world (Espinosa et al., 2019; Lovino et al., 2014; Santos et al., 2010; Vicente-Serrano, 2006b).

The method consisted of calculating the covariance matrix of the data (SPEI series) with the corresponding eigenvalues and eigenvectors. The principal components (PC) are given by linear combinations of the time series (SPEI) with maximum variance (Rencher, 2002). The number of regions were defined by the number of chosen PCs. There are several methods for finding the right number of PCs (Cangelosi and Goriely, 2007). Here the criterion selected was that they explain at least 75% of the accumulated variance, while the following PC represents less than 5%. Then, the main components were rotated (rotated principal components, RPC) using the Varimax technique (Espinosa et al., 2019) to locate more accurately the spatial patterns of drought variability, to improve their interpretation, and to redistribute the final explained variance (Vicente-Serrano, 2006b). To identify the spatial patterns of the SPEI, Pearson's correlation coefficients (r) were calculated between each RPC and the SPEI series of each CRU, resulting in smooth and gradual patterns of the SPI-12 field (Espinosa et al., 2019). When a group of centroids (CRU cells) had the high correlations r with an RPC, we delimited a new region.

In parallel, hierarchical clustering analysis was applied through the k-means method (Santos et al., 2010; Vicente-Serrano, 2006a; Wilks, 2006). The goal was to compare the number of optimal clusters with the number of PCs obtained according to the above criterion to validate the regionalization defined by the PCA method. To choose the optimal number of clusters, we used the Euclidean distances between the created clusters, which yields the lowest possible number with the greatest possible homogeneity.

Euclidean distances ensured heterogeneity between clusters, so in order to guarantee the homogeneity within clusters, the regional heterogeneity measure Hn proposed by Hosking and Wallis (1993) was used, this as a means of assessing whether the resulting regions were statistically homogeneous. A region is considered "acceptably homogeneous" if $Hn < 1$, "possibly heterogeneous" if $1 < Hn < 2$ and "definitely heterogeneous" if $Hn \geq 2$.

From this point onwards, all subsequent analyses were performed with SPEI-12 series representative of the resulting homogeneous regions, obtained by averaging all the time series contained in each of them.

2.4. Trend and persistence analysis

This step sought to analyse the temporal variability of droughts by exploring trends and their long-term persistence. On the one hand, the Mann-Kendall (MK) trend test was used to analyse whether the SPEI time series presented a significant trend, either positive or negative. The MK trend test is a rank-based non-parametric method that analyses the difference in signs between the previous and subsequent data points, using the standard normal variant (Z) (Hipel and McLeod, 1994). Although the MK trend method requires the measurements to be independent, for simplicity of analysis in the present paper we have assumed that monthly SPEI-12 meet this condition, as other studies have also done (García-Garizábal, 2017; Yao et al., 2018).

On the other hand, the Rescaled Range (R/S) statistical analysis was applied to the SPEI time series in order to quantify the long-term persistence of trends. We ascertained whether the drought trends observed to be statistically significant in the study period (past) persist in time (future), since this is related to the predictability of droughts and climate change (Koutsoyiannis, 2005, 2003). This analysis was introduced by Hurst (1956). The long-term persistence of trends in the time series is analysed by estimating the

Table 1
Climate indices considered in the correlation analysis.

Variable/data set	Period available	Data availability
Darwin sea level pressure (Darwin SLP)*	Jan 1882-now	http://cpc.ncep.noaa.gov/data/indices/darwin
Tahiti sea level pressure (Tahiti SLP)*	Jan 1882-now	http://cpc.ncep.noaa.gov/data/indices/tahiti
Southern Oscillation Index (SOI)* *	Jan 1866-now	https://psl.noaa.gov/gcos_wgsp/Timeseries/SOI/
ENSO indices (ERSSTv5): El Niño 1 + 2, El Niño 3, El Niño 4, and El Niño 3.4 *	Jan 1950-now	https://cpc.ncep.noaa.gov/data/indices/ersst5.nino.mth.81-10.ascii
Pacific Decadal Oscillation (PDO)* *	Jan 1948-Dec 2018	https://psl.noaa.gov/data/correlation/pdo.data
South Western Indian Ocean (SWIO)	Nov 1981-now	https://stateoftheocean.osmc.noaa.gov/sur/ind/swio.php
Western Tropical Indian Ocean (WTIO)* *	Jan 1870-now	https://psl.noaa.gov/gcos_wgsp/Timeseries/Data/dmiwest.had.long.data
South-eastern Tropical Indian Ocean (SETIO)* *	Jan 1870-now	https://psl.noaa.gov/gcos_wgsp/Timeseries/Data/dmieast.had.long.data
Indian Ocean dipole mode index (DMI)* *	Jan 1870-now	https://psl.noaa.gov/gcos_wgsp/Timeseries/Data/dmi.had.long.data
Tropical Northern Atlantic Index (TNA)* *	Jan 1948-now	https://psl.noaa.gov/data/correlation/tna.data
Tropical Southern Atlantic Index (TSA)* *	Jan 1948-now	https://psl.noaa.gov/data/correlation/tsa.data
North Atlantic Tropical (NAT)* **	Nov 1981-now	https://stateoftheocean.osmc.noaa.gov/sur/atl/nat.php
South Atlantic Tropical (SAT)* **	Nov 1981-now	https://stateoftheocean.osmc.noaa.gov/sur/atl/sat.php
Tropical Atlantic (TASI)* **	Nov 1981-now	https://stateoftheocean.osmc.noaa.gov/sur/atl/tasi.php
North Atlantic Oscillation (NAO)* *	Jan 1950-now	https://psl.noaa.gov/gcos_wgsp/Timeseries/Data/nao.long.data

* ; * *; * ** specifies source:
* Climate Prediction Centre of NOAA
* * Physical Sciences Laboratory of NOAA
* ** Ocean Observations Panels for Climate of NOAA

autocorrelation properties of the time series. For instance, this allows us to see whether humid years cluster in multiannual humid periods or if drought years cluster in multiannual dry periods. Such an estimation is made by means of the Hurst index (H), which is a measure of long-term persistence. The H index classifies the time series into 3 types according to their value. When $H = 0.5$, the series is completely uncorrelated and its future trend is different or equal to the past one; when $H < 0.5$, the future trend of the series will the opposite of the past series; and when $H > 0.5$, the future trend of the series will be the same as the past trend. In the latter two cases, with the lowest and highest values of H, respectively, the strength of the persistence is greatest. The steps of the computation can be seen in Gao et al. (2020).

These two analyses were applied to the monthly and annual SPEI time series averaged over the homogeneous drought regions obtained in the previous step. The annual series was assessed in this section to strengthen the limitations of using SPEI-12, as these measures can be considered non-dependent.

2.5. Relationships with large-scale climate indices

A series of large-scale climate indices were selected to analyse their possible relationships with the variability of the SPEI time series averaged over the homogeneous drought regions. The climate indices are based on the fluctuations of atmospheric pressure at sea level (SLP) of different points around the globe (Darwin SLP, Tahiti SLP, SOI and NAO indices), and the sea surface temperature (SST) of the Atlantic (TNA, TSA, NAT, SAT and TASI indices), Pacific (ENSO indices Niño 1 +2, Niño 3, Niño 4, Niño3.4 and PDO) and Indian (SWIO, WTIO, SETIO and DMI indices) oceans. The climate indices used are listed in Table 1 together with the data sources and the available period of data. For consistency with the SPEI time series, a 12-month moving average was applied to the climatic indices from 1950 to 2019, with a monthly resolution, except for PDO, SWIO, TASI, NAT and SAT, which were not available for the whole time period.

The cross-correlation method (Hair et al., 1998) was applied between the monthly and annual SPEI series and the climatic indices to quantify the strength of the link between them. Since the relationships between climatic and drought indices necessarily could not occur at the same time, we first analysed the correlation with zero lag time and then looked for the time lag (on a monthly scale) in which the correlation is greater between the two series. The time lag is associated with the early prediction of one series using the other, while the correlation coefficient indicates how strong that relationship would be. Based on the cross-correlation results, a reduced set of climate indices was selected for the next steps of the methodology.

A spectral analysis based on Fast Fourier Transform (FFT) and a cross-wavelet analysis was then performed between the monthly SPEI series and the climatic indices that showed the best correlations in the previous analysis. The idea was to further explore the relationship between these two types of indicators in each homogeneous drought region of the country.

The FFT is a well-known mathematical procedure that allows us to convert signals (time series) from the time domain to the frequency domain. This process is very useful for decomposing a time series comprising various pure frequencies (sinuses and cosines) in only a few recurring periods (Period=1/Frequency) of different lengths. Here, we looked for the periods in the SPEI and their highly correlated climatic indices. For details of the mathematical process, see Fleming et al. (2002).

Cross-wavelet analysis was initially introduced by Hudgins et al. (1993), and explores the relationships between two associated time series (in this case, the SPEI series and the climatic indices). It combines wavelet transformation with cross-spectrum analysis and can notionally capture the characteristic changes and associated oscillations of these two time series in both the time and frequency fields (Grinsted et al., 2004). A detailed description of the calculation method and applications can be found in Torrence and Compo (1997).

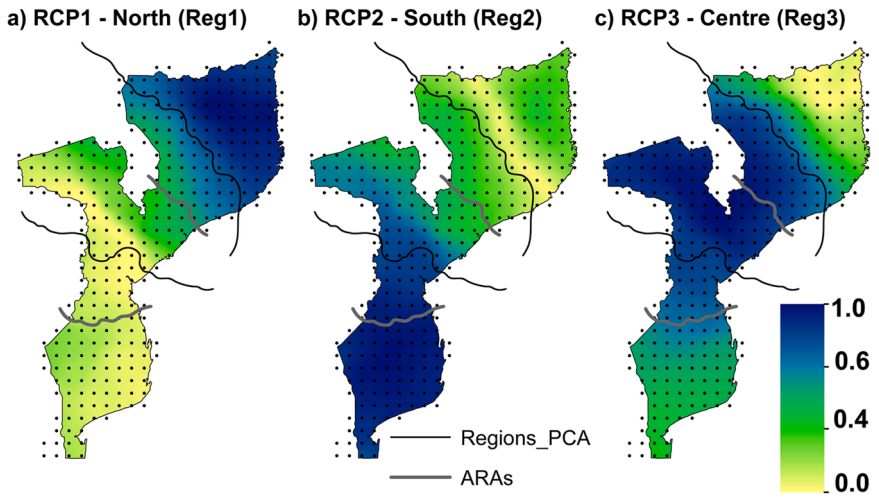

Fig. 3. Spatial distribution of the correlation coefficients between RPCs and SPEI. The continuous black lines define the regions obtained with correlations greater than 0.60. The grey lines show the three Regional Water Administrations (ARAs).

These methods have been applied in other similar studies. For example, the cross correlation method was used by Lima and AghaKouchak (2017) in Amazonia to correlate the PDSI with climate indices; Santos et al. (2010) used FFT in Portugal to determine the periodicity of droughts according to the SPI-6; and Räsänen et al. (2016) applied cross-wavelet analysis in mainland Southeast Asia to analyse the relationship between the ENSO and the Palmer drought Severity Index (PDSI, Palmer, 1965).

3. Results

3.1. Spatial distribution of droughts

Following the procedure described in Section 2.2, a total of 343 time series of SPEI values were calculated, these corresponding to the CRU coordinates presented in Fig. 2a. Each SPEI-12 time series had a length of 840 months (from 1950 to 2019).

PCA analysis was applied to the matrix that contained the times series of SPEI (with 840 rows corresponding to the length of the time series, and 343 columns corresponding to the coordinates of CRU), to transform its variables into principal components (PC) by simple linear transformations. The first PC explained a large percentage of the total variance (46.83%). The variance retained by the PC2 and PC3 were 25.17% and 7.51%, respectively. Following the proposed criteria, these three PCs were chosen for the Varimax orthogonal rotation, since together they explained 79.5% of the variance, and the part of the total variance retained by the next PC (PC4) was below 5% (4.26%). Inverse Distance Weighting (IDW) interpolation was used to plot Pearson's correlations between the three chosen RPCs and each of the 343 SPEI series (Fig. 3). This technique was applied only for plotting purposes; regionalization was based on the values at the CRU grid points. Three regions were clearly defined: North (Reg1), South (Reg2) and Centre (Reg3) following the classification obtained by the best correlations ($r > 0.60$). The coordinates of each SPEI series belonging to each RPC are listed in the supplementary materials (Table S1).

It should be noted that other temporal aggregations (SPEI-3 and SPEI-6) were also tested in this step, obtaining very similar homogeneous drought regions, as can be seen in Fig. S1 of the Supplementary materials. In what follows we used the regionalization obtained with PCA on the SPEI-12 series.

The non-hierarchical k-means clustering method was applied to the 343 SPEI time series to validate the regionalization obtained by PCA. According to PCA, a successful regionalization would be a classification into 3 groups, so here we analysed a clustering of 2, 3 and 4 regions (i.e., a variation of $\pm$ 1 with respect to the PCA result). The spatial extent of the resulting clusters is shown in Fig. 4, and the coordinates of the SPEI series belonging to each cluster are detailed in the supplementary materials (Table S1). Using the Euclidean distance between clusters method (Table 2), the classification into 2 groups (Fig. 4a) is considered inadequate, since the distance between both clusters in this configuration (26.76) is less than the distance between them (37.36) when grouped into 3 clusters (Fig. 4b). When clustering into 4 groups (Fig. 4c), the area representing cluster 1 in the 3-group division (Fig. 4b) is divided into clusters 1 and 4, while cluster 2 remains invariant. To be accepted as a better classification, the two distances (cluster 1 and 4) with respect to cluster 2 should be greater than the distance between cluster 1 and 2 when grouped into 3 clusters. Since this is not true for the distance between clusters 2 and 4 ($35.41 < 37.36$), the division into 4 clusters is rejected. Although not shown in this paper, regionalization was also performed with Ward's hierarchical clustering method (Wilks, 2006), obtaining similar results.

Based on these results, in what follows we used the regionalization obtained with PCA, which divides Mozambique into 3 homogeneous drought regions (Fig. 3). In these 3 regions, the Hn index was -0.111 for the northern region, -0.004 for the central region and -0.024 for the southern region. Thus, both heterogeneity between clusters and homogeneity within clusters was guaranteed. The SPEI series were averaged in each region (93 SPEI series on the North, 110 on the South and 140 on the Centre regions) to use in the subsequent analysis (Fig. 5).

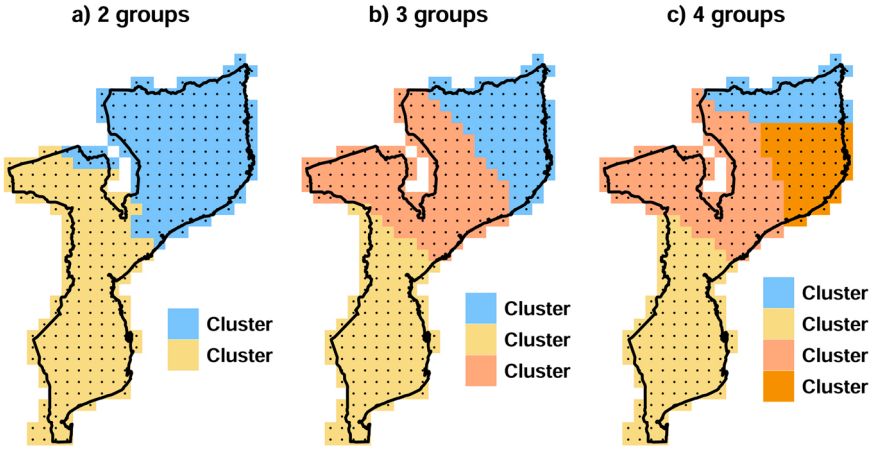

Fig. 4. Comparison of clustering in (a) two, (b) three and (c) four groups.

Table 2
Euclidean distances between clusters for the analysis with two, three and four classification groups.

	Cluster 1	Cluster 2	Cluster 3	Cluster 4
Two classification groups				
Cluster 1	0	0	0	0
Cluster 2	26.76	0	0	0
Three classification groups				
Cluster 1	0	0	0	0
Cluster 2	22.88	0	0	0
Cluster 3	37.36	26.16	0	0
Four classification groups				
Cluster 1	0	0	0	0
Cluster 2	38.32	0	0	0
Cluster 3	30.21	22.20	0	0
Cluster 4	20.44	35.41	23.80	0

3.2. Characterization of drought events

Run theory was adopted to characterize the drought events in the 3 regions previously determined (Table 3). A lower number of drought events, but of longer duration and higher severity, were found in the Centre region. On average, drought events were less intense and severe in the North. They occurred on average every 4.9 years in the North, every 4 years in the South, and every 5.9 years in the Centre region. The longest, most intense, and severest events began in 1982, 1987, 1991, 1994, 2005, 2009, and 2016; and most of them affected all three regions.

3.3. Temporal variability and persistence of droughts

The representative SPEI time series for each region are shown in Fig. 5. They are clearly non-monotonic, non-stationary according to ACF analysis (autocorrelation function, not shown here), and trend-stationary (statistical significance level of 1%) according to the KPSS test (the Kwiatkowski–Phillips–Schmidt–Shin test).

The MK test (Z index) and the R/S analysis (H index) applied to the annual and monthly SPEI time series of the three homogeneous drought regions are presented in Table 4. In all cases and regions, the trends were negative (illustrated in Fig. 5), although in the North region they were statistically non-significant at a level of 5% for the annual SPEI.

In all cases, the Hurst index (H) was greater than 0.5, which suggests that the negative long-term trends will persist in the near future. In the South and Centre regions, the H values were higher, suggesting that trends will persist with greater strength, while long-term trend persistence strength will be weak in the North region.

3.4. Identification of large-scale climate drivers

The cross-correlations and lagged cross-correlations between the proposed climate indices (Table 1) and the SPEI of the homogeneous drought regions are shown in Table 5. The best correlations are shown in the top rows of the table. The anomalies in the time series of the best-correlated climate indices are shown in Fig. 6. Most of the correlations were negative (Darwin, Niño 3.4, Niño 3, Niño 4, WTIO and SETIO), and only one was positive (SOI), indicating they are anti-phase or in-phase, respectively, relative to the SPEI.

The North region persistently showed a poor correlation with the climate indices analysed, while the strongest correlations were obtained in the South and Centre regions. In these two regions, strong correlations with the different El Niño indices were noticeable (r up to −0.59), with the higher correlations being found for the El Niño 4 and El Niño 3.4 SST indices, which showed crests around 2–3 months earlier than the negative peak of the SPEI. Another strong correlation ($r = -0.58$) with a similar time lag was found with the Darwin SLP index. Based on the above observations, El Niño 4 and Darwin indices were chosen for the spectral analysis using the FFT technique and cross-wavelet analysis.

FFT allowed us to appreciate the periodic behaviour of the monthly SPEI patterns in each homogeneous drought region, and of Darwin SLP and Niño 4 climatic indices. The periodograms are set out in Fig. 7. The results showed that climatic indices and SPEI series have a periodicity associated with high energies between 40 and 120 months (3.5 and 10 years). In the North region, periods of between 35 and 60 months (3 and 5 years) were found. These periods are consistent and similar to those reported in other studies in Africa (Oguntunde et al., 2018, 2017).

The spectral analysis of the SPEI, Darwin SLP, and El Niño 4 patterns was expanded using cross-wavelet transform (Fig. 8). Both Darwin SLP and El Niño 4 events showed strong impacts on the monthly series of SPEI, especially in the South and Centre regions, indicating that they play a relevant role in the characteristics of the evolution of droughts in Mozambique. Specifically, the positive events of Niño 4 show statistically significant negative links (confidence level 95%) with the monthly SPEI series of the South and Centre regions, with a signal of 16–128 months (1.3–10.7 years). In the North region, climatic indices did not show strong effects on the evolution of droughts (something previously seen in the low correlations); however, the statistically significant strongest signals were found for 16–64 months (1.4–5.4 years) over the entire study period. In the three regions, the energy density is higher in the periods where drought events were detected (e.g., the major drought event of 1991).

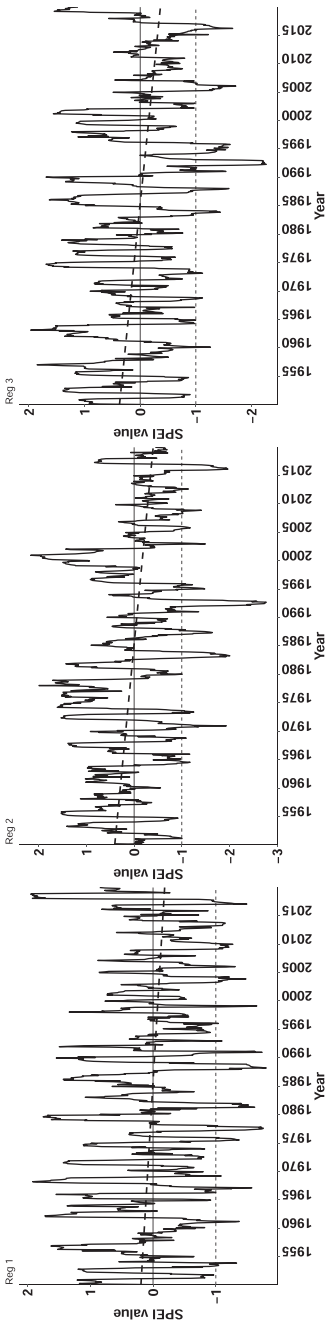

Fig. 5. SPEI time series averaged over the three regions: North (Reg1), South (Reg2) and Centre (Reg3). The thin horizontal dashed line represents the threshold considered to define a drought event while the thick dashed line represents the linear trend of the time series.

Table 3
Identification of drought events and their characteristics with run theory in the three homogeneous drought regions.

North				South				Centre			
Begin	Du	Int	Sev	Begin	Du	Int	Sev	Begin	Du	Int	Sev
06/1953	3	-1.04	-3.11	06/1964	3	-1.17	-3.31	08/1968	3	-1.12	-3.22
01/1961	3	-1.37	-3.70	10/1970	5	-1.93	-6.97	02/1973	2	-1.12	-2.19
12/1966	4	-1.57	-5.06	05/1973	4	-1.25	-4.56	09/1983	6	-1.44	-7.44
05/1975	8	-1.37	-9.50	11/1982	14	-2.01	-22.70	10/1987	5	-1.59	-6.66
04/1977	8	-1.75	-12.91	01/1987	8	-1.64	-11.07	12/1990	3	-1.54	-4.10
04/1981	9	-1.62	-12.94	10/1987	2	-1.07	-2.10	02/1992	12	-2.26	-25.54
12/1987	12	-1.80	-18.27	12/1991	15	-2.77	-32.81	03/1994	21	-1.62	-29.40
12/1990	3	-1.74	-4.72	01/1995	4	-1.48	-5.40	04/2005	16	-1.72	-21.02
12/1998	3	-1.65	-4.22	09/1995	4	-1.22	-4.35	02/2016	11	-1.66	-14.17
04/2003	12	-1.48	-13.64	12/2002	2	-1.49	-2.80				
12/2005	3	-1.31	-3.61	09/2005	4	-1.18	-4.49				
02/2009	12	-1.27	-13.62	04/2008	7	-1.41	-7.77				
04/2013	7	-1.15	-7.84	12/2015	12	-1.97	-20.47				
01/2017	5	-1.49	-6.21								
Average:	6.57	-1.47	-8.52	Average:	6.46	-1.58	-9.91	Average:	8.78	-1.56	-12.64

Table 4
Trends (Z) and Hurst index (H) of monthly and annual SPEI in the period 1950–2019 in the homogenous drought regions.

Region		Annual	Monthly
North	**Z**	-1.25[a]	-3.86
	H	–	0.69
South	**Z**	-2.32	-7.88
	H	0.61	0.74
Centre	**Z**	-2.10	-6.83
	H	0.61	0.74

[a] Trend statistically non-significant ($\rho > 0.05$)

Table 5
Cross correlations between the SPEI time series of each region and the climatic indices. r is the correlation coefficient, r_lag is the lagged correlation coefficient obtained when lag = lag_months (greater correlation) and r_annual is the correlation coefficient between the series aggregated annually.

Climatic indices	North				South				Centre			
	r	r_lag	lag months	r annual	r	r_lag	lag months	r annual	r	r_lag	lag months	r annual
Niño 4	-0.20	-0.24	4	-0.24	-0.45	-0.48	3	-0.49	-0.53	-0.56	3	-0.59
Niño 3.4	-0.17	-0.30	6	-0.23	-0.45	-0.46	2	-0.50	-0.51	-0.57	3	-0.59
Darwin	-0.14	-0.25	7	-0.21	-0.43	-0.44	2	-0.48	-0.50	-0.54	3	-0.58
Niño 3	-0.15	-0.34	7	-0.23	-0.42	-0.43	1	-0.47	-0.47	-0.53	4	-0.55
SOI	0.14	0.21	6	0.17	0.37	0.38	2	0.42	0.45	0.48	3	0.52
WTIO	-0.19	-0.20	4	-0.20	-0.38	-0.38	0	-0.40	-0.41	-0.41	0	-0.43
SETIO	-0.28	-0.29	2	-0.24	-0.32	-0.40	-6	-0.35	-0.38	-0.41	-3	-0.39
Niño 1 + 2	-0.12	-0.29	8	-0.19	-0.31	-0.31	-1	-0.36	-0.35	-0.40	4	-0.42
Tahiti	0.10	-0.18	20	0.09	0.27	0.27	1	0.29	0.33	0.35	2	0.36
PDO[a]	-0.20	-0.21	3	-0.21	-0.22	-0.28	-9	-0.25	-0.30	-0.30	-1	-0.32
SWIO[b]	-0.13	-0.13	-2	-0.10	-0.17	-0.20	-5	-0.19	-0.24	-0.26	-3	-0.23
NAO	0.17	0.18	1	0.16	-0.22	-0.29	4	-0.26	-0.22	-0.33	5	-0.32
TASI[b]	-0.14	-0.24	-10	-0.17	0.30	0.30	-1	0.31	0.18	0.36	11	0.22
TNA	-0.24	-0.24	-2	-0.22	-0.10	-0.20	17	-0.12	-0.17	-0.18	-2	-0.15
DMI	0.05	-0.21	-11	-0.02	-0.17	-0.30	5	-0.21	-0.16	-0.26	5	-0.22
NAT[b]	-0.27	-0.28	-1	-0.26	0.08	0.18	7	0.09	-0.13	0.21	11	-0.09
SAT[b]	-0.12	-0.21	-10	-0.16	0.24	0.27	-3	0.24	0.12	0.29	11	0.13
TSA	-0.12	-0.13	3	-0.14	-0.07	-0.25	-19	-0.09	-0.07	-0.22	-16	-0.08

[a] Period Jan1950-Dec2018.
[b] Period Jan1982-Dec2019.

4. Discussion

The above results provide new insights into the spatial and temporal patterns of drought in Mozambique, and their relationship with the large-scale climate variability.

The resulting drought regionalisation differs from other divisions created for other management purposes (FEWS NET

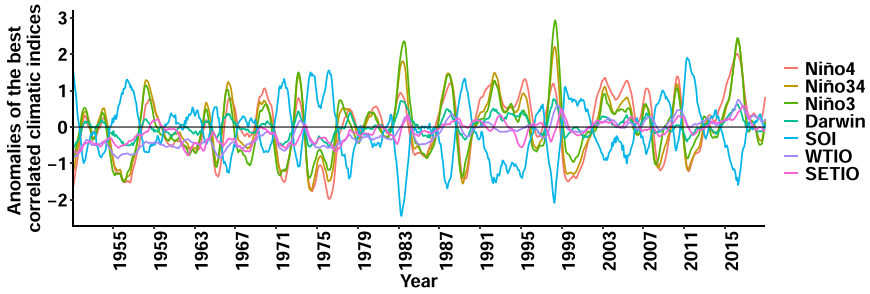

Fig. 6. Anomalies of the best correlated climatic indices with the SPEI time series in the period 1950–2019.

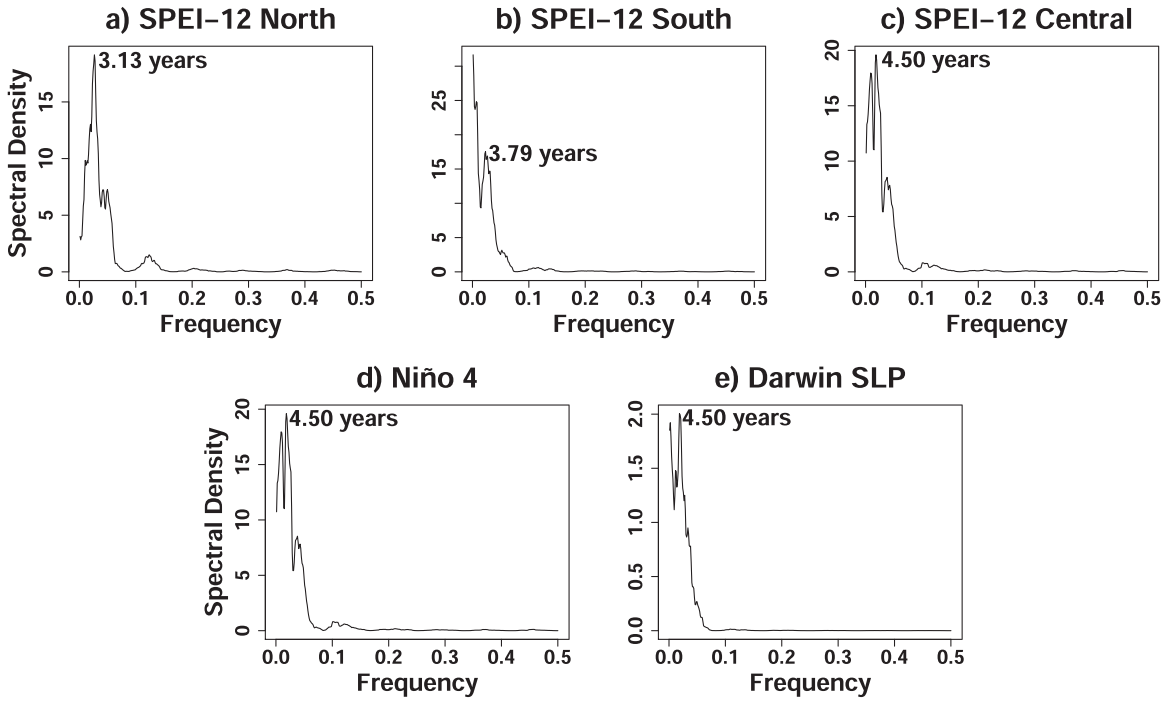

Fig. 7. Fast Fourier Transform of monthly SPEI time series of a) North, b) South, c) Centre regions, d) the climatic index Niño 4, and e) the climatic index Darwin SLP. Peaks have been transformed to years.

Moçambique, 2014; INGC, 2009). As shown in Fig. 3, the regions as defined also do not entirely coincide with those used by the Mozambican government for water resources management (ARAs), although the spatial positioning patterns (North, Centre, and South) are maintained. The use of the proposed divisions as drought management areas would allow for more appropriate regional strategies for assessing, monitoring, and responding to drought (Wilhite et al., 2000). The most important drought events identified in these regions have been listed and coincided with the major ones at the national level.

The trends observed in the SPEI series were consistent with the trends found for the SPEI input variables (i.e., precipitation and temperature) shown in Fig. 2b and c., where trends were positive for temperature and negative for precipitation. In addition, these findings are in line with similar ones reported by Jury (2013), who used satellite sensor data to analyse climate trends in southern Africa and found that temperature and precipitation trends were positive and negative, respectively, over the period 1980–2010 in Mozambique as a whole. On the other hand, the persistence analysis points to an increase in the incidence of droughts throughout the country. Although these results should be taken with caution due to the climate system complexity, they further highlight the need for the development of drought forecasting tools and more specific, in-depth studies on drought variability in the homogeneous regions. These results are consistent with those found at the continental level and in other regions of Africa (Masih et al., 2014; Rouault and Richard, 2005), and with the variations seen in recent years on precipitation and temperature in Mozambique (Jury, 2013; Uele et al., 2017).

Relationships found between droughts and El Niño 4 and El Niño 3.4 SST indices agree with those described in Manhique et al. (2011) for southern Africa and Mozambique as a whole, and in Manatsa et al. (2008a) for the neighbouring tropical country of Zimbabwe. The strong climatic influence of the Darwin SLP index was also found by Manatsa et al. (2008b) in Zimbabwe. Other

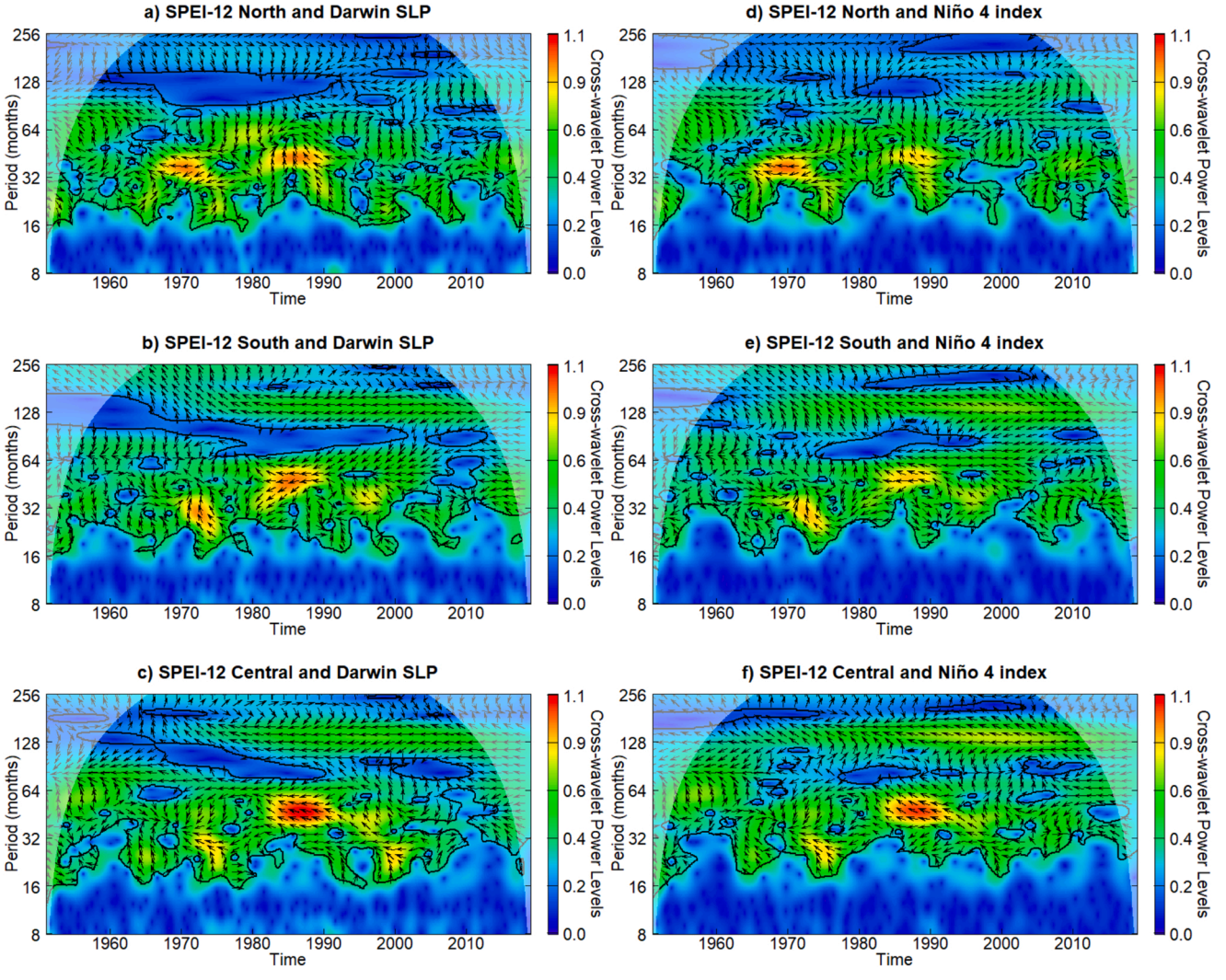

Fig. 8. Cross-wavelet transform between SPEI of a) North, b) South, c) Centre regions and Darwin PSL climatic index; and of d) North, e) South, f) Centre regions and the Niño 4 climatic index. The y-axis is equivalent to the periods defined with the FTT (Period = 1/Frequency); the coloured bar denotes the energy density (red plus high energy density); the 5% confidence level against red noise is shown in an outline with the thick black line; and the relative phase relationship is represented with arrows (with the anti-phase pointing to the left, the in-phase pointing to the right).

tropical regions of the world have also found El Niño 4 and Darwin to be drought triggers (D'Arrigo and Smerdon, 2008; Gu et al., 2020; Lyon and Barnston, 2005), so these (and following) results are also of hydrological interest for countries located in these climatic regions.

The periodic behaviour of the monthly SPEI patterns according to FTT match those reported in Section 3.2., and coincide with the historical drought records documented in EM-DAT (2020) and Masih et al. (2014). Thus, these results are of great importance, as well as being novel for the region. The periodicity found in the El Niño 4 (the same oscillation period was observed for Darwin SPL) index is consistent with the widely accepted 3–7 year period (McPhaden et al., 1998).

The results of the spectral analysis consistently point to an anti-phase relationship between the drought events detected by SPEI and the climatic indices Darwin SLP and El Niño 4 in the South and Centre regions. The North region showed a poor relationship with the climatic indicators. In this region of the country, drought events are less intense and severe, although the number of events is higher. This may be explained by the relationship between the Temperate Tropical Depressions and ENSO. This relationship affects the precipitation patterns in Southeast Africa, making ENSO less influential in the North of Mozambique and meaning that it is a wetter area than the rest of the country (Manhique et al., 2011).

These climate indices could be used in drought forecasting models as predictors of drought in Mozambique, with a lead time of 2–3 months based on the lagged correlations. Such a lead time would enable the establishment of preventive measures against possible upcoming droughts (e.g., accumulating water in reservoirs, prioritizing water use for different uses, etc.). In this way, a forecasting model could be employed to infer the probability and intensity of drought events in the short-term future, relying on past values of the climate indices (Hao et al., 2018), and allowing actions to be implemented when a drought is expected.

5. Conclusions

The main objective of this study was to investigate the spatio-temporal characteristics of droughts and their relationships with possible predictors of the phenomenon in Mozambique. Although Mozambique is very prone to droughts and suffers continuously from their effects, it does not have the necessary management tools to monitor and predict the phenomenon. The proposed five-step methodology consists of several methods organised in a coherent way for use in Mozambique or in any other region (country or river basin) that requires a first assessment of the spatio-temporal characteristics of droughts. Here, efforts have been made to adapt the methodology specifically to Mozambique, where local meteorological and hydrological monitoring data are extremely limited.

The monthly SPEI-12 was calculated as an indicator of drought from 1950 to 2019 at a high resolution (0.5°). Principal Component Analysis with the Varimax rotation method was used to define 3 homogeneous drought regions located in the North, South, and Centre of the country. This regionalization was validated with hierarchical and non-hierarchical clustering methods. The regions as delimited do not coincide entirely with those identified by the Mozambican National Directorate of Water but are preferable for drought monitoring and management.

Based on run theory, the South and Centre regions are the ones that have presented the most intense and severe drought events in the past. A statistically significant trend towards a higher incidence of droughts was found in the three regions and Rescale Range analysis suggests that this trend might persist in the near future. This section presented valuable information for Mozambique on the temporal variability of droughts. However, given the limitations derived from the use of SPEI-12, it would be advisable to consider additional time scales in future studies to gain further insights into the temporal patterns of drought in each region.

Strong correlations between two climatic indices—El Niño 4 (ENSO) and Darwin SLP—and droughts were found in the South and Centre regions, with a time lag of 2–3 months. These climate indices are representative drought triggers in tropical regions of the world such as Mozambique. With the FFT technique, it was found that the periods of SPEI and these two climate indices have a similar periodicity of between 3 and 8 years, this being a novel statement with reference to Mozambique. Spectral analysis by means of cross-wavelet transform confirmed that SPEI and El Niño 4 and Darwin SLP are strongly related in anti-phase for periods between 1.4 and 10.4 years. These climate indices could thus be used to develop a drought forecasting system, providing sufficient lead time to establish prevention strategies.

In summary, this study has provided an understanding of the spatial and temporal distribution of droughts in Mozambique. The results are of great potential use for Mozambique's regional water administrations towards developing drought contingency plans. Simplified management regions have been defined, characterised, and strongly related to potential drought predictors. The proposed methodology can be used elsewhere in the world; however, given its limitations and the large number of topics it covers, certain limitations will need to be considered in future studies.

CRediT authorship contribution statement

This research is part of the PhD thesis of Araneda-Cabrera R. Both Bermúdez M. and Puertas J. were thesis supervisors. **Ronnie J. Araneda-Cabrera:** Conceptualization, Methodology, Software, Formal analysis, Investigation, Data Curation, Writing – original draft, Visualization. **María Bermudez:** Conceptualization, Validation, Formal analysis, Writing – review & editing, Supervision. **Jerónimo Puertas:** Conceptualization, Resources, Writing – review & editing, Supervision.

Declaration of Competing Interest

The authors declare that they have no known competing financial interests or personal relationships that could have appeared to influence the work reported in this paper.

Acknowledgments

Ronnie Araneda gratefully acknowledges financial support from the Spanish Regional Government of Galicia (Xunta de Galicia) and the European Union through the Predoctoral Grant reference ED481A-2018/162. María Bermúdez was supported by the European Union H2020 research and innovation program under the Marie Skłodowska-Curie Grant Agreement No. 754446 and the Research and Transfer Fund of the University of Granada - Athenea3i. The authors would like to thank Manuel Alvarez and Victor Penas for their comments and support during the development of the study.

Appendix A. Supporting information

Supplementary data associated with this article can be found in the online version at doi:10.1016/j.ejrh.2021.100938.

References

Abatzoglou, J.T., Dobrowski, S.Z., Parks, S.A., Hegewisch, K.C., 2018. TerraClimate, a high-resolution global dataset of monthly climate and climatic water balance from 1958-2015. Sci. Data 5, 1–12. https://doi.org/10.1038/sdata.2017.191.

Agutu, N.O., Awange, J.L., Zerihun, A., Ndehedehe, C.E., Kuhn, M., Fukuda, Y., 2017. Assessing multi-satellite remote sensing, reanalysis, and land surface models' products in characterizing agricultural drought in East Africa. Remote Sens. Environ. 194, 287–302. https://doi.org/10.1016/j.rse.2017.03.041.

Alley, W.M., 1984. The palmer drought severity index: limitations and assumptions. J. Clim. Appl. Meteorol. 23, 1100–1109. https://doi.org/10.1175/1520-0450(1984)023<1100:TPDSIL>2.0.CO;2.

Araneda-Cabrera, R.J., Bermudez, M., Puertas, J., 2021a. Benchmarking of drought and climate indices for agricultural drought monitoring in Argentina. Sci. Total Environ. 790, 148090 https://doi.org/10.1016/j.scitotenv.2021.148090.

Araneda-Cabrera, R.J., Bermúdez, M., Puertas, J., 2021b. Assessment of the performance of drought indices for explaining crop yield variability at the national scale: methodological framework and application to Mozambique. Agric. Water Manag. 246. https://doi.org/10.1016/j.agwat.2020.106692.

Araneda-Cabrera, R.J., Bermúdez, M., Puertas, J., 2020. Unified framework for drought monitoring and assessment in a transboundary river basin. In: Uijttewaal, W., Franca, M., Valero, D., Chavarrias, V., Arbós, C., Schielen, R., Crosato, A. (Eds.), River Flow 2020. Taylor & Francis Group, London, pp. 1081–1086. https://doi.org/10.1201/b22619.

Ayantobo, O.O., Li, Y., Song, S., Yao, N., 2017. Spatial comparability of drought characteristics and related return periods in mainland China over 1961–2013. J. Hydrol. 550, 549–567. https://doi.org/10.1016/j.jhydrol.2017.05.019.

Begueria, S., Vicente-Serrano, S.M., 2017. Package 'SPEI'. version 1.7. ⟨ftp://tucows.icm.edu.pl/packages/cran/web/packages/SPEI/SPEI.pdf⟩. A case study Birkoor Kortigiri Mandals. https://doi.org/10.1175/2009JCLI2909.1.http.

Bolar, K., 2019. Package 'STAT'. version 0.1.0. https://cran.r-project.org/web/packages/STAT/STAT.pdf.

Borchers, H.W., 2019. Package 'pracma'. version 2.2.9. http://mirrors.ucr.ac.cr/CRAN/web/packages/pracma/pracma.pdf.

Bryant, E.A., Head, L.M., Morrison, R., 2005. Planning for Natural Hazards — How Can We Mitigate the Impacts ?, in: R.J. Morrison, S. Quin and E.A. Bryant (Eds.), Planning for Natural Hazards — How Can We Mitigate the Impacts?, Proceedings of a Symposium, 2–5 February 2005, University of Wollongong, GeoQuEST Research Centre, 2005, 1–11.

Cangelosi, R., Goriely, A., 2007. Component retention in principal component analysis with application to cDNA microarray data. Biol. Direct. 2, 1–21. https://doi.org/10.1186/1745-6150-2-2.

Conselho de Ministros, 2020. BR No 160 de 20.08.20, Boletim da República - I Serie. Publicação oficial da República de Moçambique. Maputo, Mozambique. https://www.inm.gov.mz/pt-br/content/br-n%C2%BA-160-de-200820-boletim-da-rep%C3%BAblica-i-serie.

Dutra, E., Di Giuseppe, F., Wetterhall, F., Pappenberger, F., 2013. Seasonal forecasts of droughts in African basins using the standardized precipitation index. Hydrol. Earth Syst. Sci. 17, 2359–2373. https://doi.org/10.5194/hess-17-2359-2013.

D'Arrigo, R., Smerdon, J.E., 2008. Tropical climate influences on drought variability over Java, Indonesia. Geophys. Res. Lett. 35, 1–5. https://doi.org/10.1029/2007GL032589.

Easterling, D.R., 2013. Global data sets for analysis of climate extremes. In: Water Science and Technology Library (Ed.), Global Data Sets for Analysis of Climate Extremes. Springer, Dordrecht, pp. 347–361. https://doi.org/10.1007/978-94-007-4479-0_12.

EM-DAT, 2020. The Emergency Events Database, Universite catholique de Louvain, Brussels, Belgium. http://www.emdat.be/, (Accessed November 2020).

Eriksen, S., Silva, J.A., 2009. The vulnerability context of a savanna area in Mozambique: household drought coping strategies and responses to economic change. Environ. Sci. Policy 12, 33–52. https://doi.org/10.1016/j.envsci.2008.10.007.

Espinosa, L.A., Portela, M.M., Rodrigues, R., 2019. Spatio-temporal variability of droughts over past 80 years in Madeira Island. J. Hydrol. Reg. Stud. 25, 100623 https://doi.org/10.1016/j.ejrh.2019.100623.

FEWS NET Moçambique, 2014. MOÇAMBIQUE Descrição das zonas de Formas de Vida, USAID https://fews.net/sites/default/files/documents/reports/MZ%20LHdescriptions%202013%20pt.pdf.

Fleming, S.W., Marsh Lavenue, A., Aly, A.H., Adams, A., 2002. Practical applications of spectral analysis of hydrologic time series. Hydrol. Process. 16, 565–574. https://doi.org/10.1002/hyp.523.

Gao, X., Dong, S., Li, S., Xu, Y., Liu, S., Zhao, H., Yeomans, J., Li, Y., Shen, H., Wu, S., Zhi, Y., 2020. Using the random forest model and validated MODIS with the field spectrometer measurement promote the accuracy of estimating aboveground biomass and coverage of alpine grasslands on the Qinghai-Tibetan Plateau. Ecol. Indic 112. https://doi.org/10.1016/j.ecolind.2020.106114.

García-Garizábal, I., 2017. Rainfall variability and trend analysis in coastal arid Ecuador. Int. J. Climatol. 37, 4620–4630. https://doi.org/10.1002/joc.5110.

Gouhier, T.C., Grinsted, A., Simko, V., 2016. Package 'biwavelet'. version 0.20.11. https://mran.revolutionanalytics.com/snapshot/2018-01-06/web/packages/biwavelet/biwavelet.pdf.

Grinsted, A., Moore, J.C., Jevrejeva, S., 2004. Application of the cross wavelet transform and wavelet coherence to geophysical time series. Nonlinear Process. Geophys. 11, 561–566. https://doi.org/10.5194/npg-11-561-2004.

Guttman, N.B., 1999. Accepting the standardized precipitation index: a calculation algorithm. JAWRA J. Am. Water Resour. Assoc. 35, 311–322. https://doi.org/10.1111/j.1752-1688.1999.tb03592.x.

Guttman, N.B., 1998. Comparing the palmer drought index and the standardized precipitation index. J. Am. Water Resour. Assoc. 34, 113–121. https://doi.org/10.1111/j.1752-1688.1998.tb05964.x.

Gu, Y., Liu, H., Traoré, D.D., Huang, C., 2020. ENSO-related droughts and ISM variations during the last millennium in tropical southwest China. Clim. Dyn. 54, 649–659. https://doi.org/10.1007/s00382-019-05019-1.

Hagenlocher, M., Meza, Isabel, Carl Anderson, Annika, Min, Fabrice G., Renaud, Y., Walz, S.S., Sebesvari, Z., 2019. Drought vulnerability and risk assessments: state of the art, persistent gaps, and research agenda. Environ. Res. Lett. 4. https://doi.org/10.1088/1748-9326/ab225d.

Hair, J.F., Black, W.C., Babin, B.J., Anderson, R.E., 1998. Multivariate Data Analysis, seventh ed. Pearson Prentice Hall, Englewood Cliffs, New Jersey, USA.

Hao, Z., Singh, V.P., Xia, Y., 2018. Seasonal drought prediction: advances, challenges, and future prospects. Rev. Geophys. 56, 108–141. https://doi.org/10.1002/2016RG000549.
Harris, I., Jones, P.D., Osborn, T.J., Lister, D.H., 2014. Updated high-resolution grids of monthly climatic observations - the CRU TS3.10 Dataset. Int. J. Climatol. 34, 623–642. https://doi.org/10.1002/joc.3711.
Hipel, K.W., McLeod, A.I., 1994. Time Series Modelling of Water Resources and Environmental Systems. Elsevier Science, New York.
Hosking, J.R.M., Wallis, J.R., 1993. Some statistics useful in regional frequency analys. Water Resour. Res. 29, 271–281.
Huang, S., Huang, Q., Leng, G., Liu, S., 2016. A nonparametric multivariate standardized drought index for characterizing socioeconomic drought: a case study in the Heihe River Basin. J. Hydrol. 542, 875–883. https://doi.org/10.1016/j.jhydrol.2016.09.059.
Hudgins, L., Friehe, C.A., Mayer, M.E., 1993. Wavelet transforms and atmopsheric turbulence. Phys. Rev. Lett. 71, 3279–3282. https://doi.org/10.1103/PhysRevLett.71.3279.
Hurst, H.E., 1956. Methods of using long-term storage in reservoirs., in: Proceedings of the Institution of Civil Engineers 5 (5). pp. 519–543. https://doi.org/https://doi.org/10.1680/iicep.1956.11503.
INGC, 2009. In: van Logchem, B., Brito, R. (Eds.), Synthesis report. INGC Climate Change Report: Study on the impact of climate change on disaster risk in Mozambique. INGC, Mozambique. Maputo, Mozambique. http://pure.iiasa.ac.at/id/eprint/9007/.
Inguane, R., Gallego-Ayala, J., Juízo, D., 2014. Decentralized water resources management in Mozambique: Challenges of implementation at the river basin level. Phys. Chem. Earth 67–69, 214–225. https://doi.org/10.1016/j.pce.2013.08.004.
IPCC, 2014. In: Edenhofer, O., Pichs-Madruga, R., Sokona, Y., Farahani, E., Kadner, S., Seyboth, K., Adler, A. (Eds.), Climate. Cambridge University Press, Cambridge, United Kingdom and New York, NY, USA.
Jehanzaib, M., Kim, T.W., 2020. Exploring the influence of climate change-induced drought propagation on wetlands. Ecol. Eng. 149, 105799 https://doi.org/10.1016/j.ecoleng.2020.105799.
Jehanzaib, M., Shah, S.A., Yoo, J., Kim, T.W., 2020. Investigating the impacts of climate change and human activities on hydrological drought using non-stationary approaches. J. Hydrol. 588, 125052 https://doi.org/10.1016/j.jhydrol.2020.125052.
Jury, M.R., 2013. Climate trends in southern Africa. S. Afr. J. Sci. 109, 1–11. https://doi.org/10.1590/sajs.2013/980.
El Kenawy, A.M., McCabe, M.F., Vicente-Serrano, S.M., López-Moreno, J.I., Robaa, S.M., 2016. Cambios en la frecuencia y severidad en las sequías hidrológicas de Etiopía entre 1960 y 2013. Cuad. Investig. Geogr. 42, 145–166. https://doi.org/10.18172/cig.2931.
Kim, T.W., Jehanzaib, M., 2020. Drought risk analysis, forecasting and assessment under climate change. Water 12, 1–7. https://doi.org/10.3390/W12071862.
Koutsoyiannis, D., 2005. Hydrologic Persistence and The Hurst Phenomenon, in: Water Encyclopedia. pp. 210–221. https://doi.org/10.1002/047147844x.sw434.
Koutsoyiannis, D., 2003. Climate change, the Hurst phenomenon, and hydrological statistics. Hydrol. Sci. J. 48, 3–24. https://doi.org/10.1623/hysj.48.1.3.43481.
Lima, C.H.R., AghaKouchak, A., 2017. Droughts in Amazonia: spatiotemporal variability, teleconnections, and seasonal predictions. Water Resour. Res. 53, 10824–10840. https://doi.org/10.1002/2016WR020086.
Liu, S., Shi, H., Sivakumar, B., 2020. Socioeconomic drought under growing population and changing climate: a new index considering the resilience of a regional water resources system. J. Geophys. Res. Atmos. 125. https://doi.org/10.1029/2020JD033005.
Lovino, M., García, N.O., Baethgen, W., 2014. Spatiotemporal analysis of extreme precipitation events in the Northeast region of Argentina (NEA). J. Hydrol. Reg. Stud. 2, 140–158. https://doi.org/10.1016/j.ejrh.2014.09.001.
Lyon, B., Barnston, A.G., 2005. ENSO and the spatial extent of interannual precipitation extremes in tropical land areas. J. Clim. 18, 5095–5109. https://doi.org/10.1175/JCLI3598.1.
Macarringue, L.S., Sano, E.E., Chaves, J.M., Bolfe, E.L., 2017. Considerações Sobre Precipitação, Relevo E Solos E Análise Do Potencial De Expansão Agrícola Da Região Norte De Moçambique. Soc. Nat. 29, 109–122. https://doi.org/10.14393/sn-v29n1-2017-7.
Manatsa, D., Chingombe, W., Matarira, C.H., 2008a. The impact of the positive Indian Ocean dipole on Zimbabwe droughts. Int. J. Climatol 28. https://doi.org/10.1002/joc.
Manatsa, D., Chingombe, W., Matsikwa, H., Matarira, C.H., 2008b. The superior influence of Darwin Sea level pressure anomalies over ENSO as a simple drought predictor for Southern Africa. Theor. Appl. Climatol. 92, 1–14. https://doi.org/10.1007/s00704-007-0315-3.
Manhique, A.J., Reason, C.J.C., Rydberg, L., Fauchereau, N., 2011. ENSO and Indian Ocean sea surface temperatures and their relationships with tropical temperate troughs over Mozambique and the Southwest Indian Ocean. Int. J. Climatol. 31, 1–13. https://doi.org/10.1002/joc.2050.
Masih, I., Maskey, S., Mussá, F.E.F., Trambauer, P., 2014. A review of droughts on the African continent: a geospatial and long-term perspective. Hydrol. Earth Syst. Sci. 18, 3635–3649. https://doi.org/10.5194/hess-18-3635-2014.
McKee, T.B., Doesken, N.J., Kleist, J., 1993. The Relationship of Drought Frequency and Duration to Time Scales, Paper Presented at 8th Conference on Applied Climatology. American Meteorological Society, Anaheim, CA. https://doi.org/10.1088/1755-1315/5.
McPhaden, M.J., Busalacchi, A.J., Cheney, R., Donguy, J.R., Gage, K.S., Halpern, D., Ji, M., Julian, P., Meyers, G., Mitchum, G.T., Niiler, P.P., Picaut, J., Reynolds, R. W., Smith, N., Takeuchi, K., 1998. The Tropical Ocean-Global Atmosphere observing system: a decade of progress. J. Geophys. Res. Ocean. 103, 14169–14240. https://doi.org/10.1029/97jc02906.
Meresa, H.K., Osuch, M., Romanowicz, R., 2016. Hydro-meteorological drought projections into the 21-st century for selected polish catchments. Water 8. https://doi.org/10.3390/w8050206.
Mishra, A.K., Singh, V.P., 2011. Drought modeling - a review. J. Hydrol. 403, 157–175. https://doi.org/10.1016/j.jhydrol.2011.03.049.
MunichRE, 2018. NatCatSERVICE.
Nam, W.H., Hayes, M.J., Svoboda, M.D., Tadesse, T., Wilhite, D.A., 2015. Drought hazard assessment in the context of climate change for South Korea. Agric. Water Manag. 160, 106–117. https://doi.org/10.1016/j.agwat.2015.06.029.
Oguntunde, P.G., Abiodun, B.J., Lischeid, G., 2017. Impacts of climate change on hydro-meteorological drought over the Volta Basin, West Africa. Glob. Planet. Change 155, 121–132. https://doi.org/10.1016/j.gloplacha.2017.07.003.
Oguntunde, P.G., Lischeid, G., Abiodun, B.J., 2018. Impacts of climate variability and change on drought characteristics in the Niger River Basin, West Africa. Stoch. Environ. Res. Risk Assess. 32, 1017–1034. https://doi.org/10.1007/s00477-017-1484-y.
Osbahr, H., Twyman, C., Neil Adger, W., Thomas, D.S.G., 2008. Effective livelihood adaptation to climate change disturbance: scale dimensions of practice in Mozambique. Geoforum 39, 1951–1964. https://doi.org/10.1016/j.geoforum.2008.07.010.
Palmer, W.C., 1965. Meteorological Drought, Research paper no. 45. US Weather Bur. Washington, DC. p-and-precip/drought/docs/palmer.pdf 58.
Patt, A.G., Schröter, D., 2008. Perceptions of climate risk in Mozambique: Implications for the success of adaptation strategies. Glob. Environ. Chang. 18, 458–467. https://doi.org/10.1016/j.gloenvcha.2008.04.002.
Pohlert, T., 2020. Package 'trend'. version 1.1.4. https://cran.r-project.org/web/packages/trend/trend.pdf.
Quiring, S.M., Papakryiakou, T.N., 2003. An evaluation of agricultural drought indices for the Canadian prairies. Agric. For. Meteorol. 118, 49–62. https://doi.org/10.1016/S0168-1923(03)00072-8.
Räsänen, T.A., Lindgren, V., Guillaume, J.H.A., Buckley, B.M., Kummu, M., 2016. On the spatial and temporal variability of ENSO precipitation and drought teleconnection in mainland Southeast Asia. Clim. Past 12, 1889–1905. https://doi.org/10.5194/cp-12-1889-2016.
Rencher, A.C., 2002. Methods of Multivariate Analysis, second. John Wiley & Sons. https://www.ipen.br/biblioteca/slr/cel/0241.
Rivera, J.A., Otta, S., Lauro, C., Zazulie, N., 2021. A decade of hydrological drought in Central-Western Argentina. Front. Water 3, 1–20. https://doi.org/10.3389/frwa.2021.640544.
Rouault, M., Richard, Y., 2005. Intensity and spatial extent of droughts in southern Africa. Geophys. Res. Lett. 32, 2–5. https://doi.org/10.1029/2005GL022436.
RStudio Team, 2016. Integrated Development Environment for R. RStudio, Inc., Boston, MA URL http://www.rstudio.com/.
Rudolf, B., Becker, A., Schneider, U., 2011. New GPCC full data reanalysis version 5 provides high-quality gridded monthly precipitation data. GEWEX News 2010, 2009–2010.

Santos, J.F., Pulido-Calvo, I., Portela, M.M., 2010. Spatial and temporal variability of droughts in Portugal. Water Resour. Res. 46, 1–13. https://doi.org/10.1029/2009WR008071.
Seibert, M., Merz, B., Apel, H., 2017. Seasonal forecasting of hydrological drought in the Limpopo Basin: a comparison of statistical methods. Hydrol. Earth Syst. Sci. 21, 1611–1629. https://doi.org/10.5194/hess-21-1611-2017.
Sheffield, J., Wood, E.F., 2012. Drought: past problems and future scenarios. Drought Past Probl. Futur. Scenar. 9781849775, 1–234. https://doi.org/10.4324/9781849775250.
Stagge, J.H., Kingston, D.G., Tallaksen, L.M., Hannah, D.M., 2017. Observed drought indices show increasing divergence across Europe. Sci. Rep. 7, 1–10. https://doi.org/10.1038/s41598-017-14283-2.
Svodova, M., Funchs, B.A., Integrated Drought Management Programme (IDMP), 2016. Handbook of Drought Indicators and Indices. Drought Mitigation Center Faculty Publications, p. 117. https://doi.org/10.1007/s00704-016-1984-6.
Torrence, C., Compo, G.P., 1997. A Practical Guide to Wavelet Analysis. American Meteorological Society. https://doi.org/10.1016/j.biopha.2017.10.142.
Trambauer, P., Maskey, S., Werner, M., Pappenberger, F., Van Beek, L.P.H., Uhlenbrook, S., 2014. Identification and simulation of space-time variability of past hydrological drought events in the Limpopo River basin, southern Africa. Hydrol. Earth Syst. Sci. 18, 2925–2942. https://doi.org/10.5194/hess-18-2925-2014.
Trambauer, P., Werner, M., Winsemius, H.C., Maskey, S., Dutra, E., Uhlenbrook, S., 2015. Hydrological drought forecasting and skill assessment for the Limpopo River basin, southern Africa. Hydrol. Earth Syst. Sci. 19, 1695–1711. https://doi.org/10.5194/hess-19-1695-2015.
Trapletti, A., Hornik, K., LeBaron, B., 2020. Package ‘ tseries ’. version 0.10–48. https://cran.r-project.org/web/packages/tseries/tseries.pdf.
Uele, D.I., Lyra, G.B., de Oliveira Júnior, J.F., 2017. Variabilidade Espacial e Intranual das Chuvas na Região Sul de Moçambique, África Austral. Rev. Bras. Meteorol. 32, 473–484. https://doi.org/10.1590/0102-77863230013.
Vicente-Serrano, S.M., 2006a. Spatial and temporal analysis of droughts in the Iberian Peninsula (1910-2000). Hydrol. Sci. J. 51, 83–97. https://doi.org/10.1623/hysj.51.1.83.
Vicente-Serrano, S.M., 2006b. Differences in spatial patterns of drought on different time scales: an analysis of the Iberian Peninsula. Water Resour. Manag. 20, 37–60. https://doi.org/10.1007/s11269-006-2974-8.
Vicente-Serrano, S.M., Beguería, S., López-Moreno, J.I., 2010a. A multiscalar drought index sensitive to global warming: the standardized precipitation evapotranspiration index. J. Clim. 23, 1696–1718. https://doi.org/10.1175/2009JCLI2909.1.
Vicente-Serrano, S.M., Beguería, S., López-Moreno, J.I., Angulo, M., El Kenawy, A., 2010b. A new global 0.5° gridded dataset (1901–2006) of a multiscalar drought index: comparison with current drought index datasets based on the palmer drought severity index. J. Hydrometeorol. 11, 1033–1043. https://doi.org/10.1175/2010JHM1224.1.
Vicente-Serrano, S.M., Beguería, S., Lorenzo-Lacruz, J., Camarero, J.J., López-Moreno, J.I., Azorin-Molina, C., Revuelto, J., Morán-Tejeda, E., Sanchez-Lorenzo, A., 2012. Performance of drought indices for ecological, agricultural, and hydrological applications. Earth Interactions, p. 16. https://doi.org/10.1175/2012EI000434.1.
Wilhite, D.A., Sivakumar, M.V.K., Wood, D.A., 2000. Early Warning Systems for Drought Preparedness and Drought Management, in: Proceedings of an Expert Group Meeting Held 5–7 September, 2000, in Lisbon, Portugal. http://Www.Wamis.Org/Agm/Pubs/Agm2/Agm02.Pdf. pp. 182–199.
Wilks, D.S., 2006. Statistical Methods in the Atmospheric Sciences, second ed. Academic Press, San Diego, CA.
, 2006WMO, Drought monitoring and early warning: concepts, progress and future challenges World Meteorol. Organ. 2006 24.
Yao, N., Li, Y., Lei, T., Peng, L., 2018. Drought evolution, severity and trends in mainland China over 1961–2013. Sci. Total Environ. 616–617, 73–89. https://doi.org/10.1016/j.scitotenv.2017.10.327.
Yevjevich, V., 1969. An objective approach to definitions and investigations of continental hydrologic droughts. J. Hydrol. https://doi.org/10.1016/0022-1694(69)90110-3.
Zambreski, Z.T., Lin, X., Aiken, R.M., Kluitenberg, G.J., Pielke, R.A., 2018. Identification of hydroclimate subregions for seasonal drought monitoring in the U.S. Great Plains. J. Hydrol. 567, 370–381. https://doi.org/10.1016/j.jhydrol.2018.10.013.
Zeleke, T.T., Giorgi, F., Diro, G.T., Zaitchik, B.F., 2017. Trend and periodicity of drought over Ethiopia. Int. J. Climatol. 37, 4733–4748. https://doi.org/10.1002/joc.5122.
Zelenhasić, E., Salvai, A., 1987. A method of streamflow drought analysis. Water Resour. Res. 23, 156–168. https://doi.org/10.1029/WR023i001p00156.